第45卷第1期
2026年2月

红外与毫米波学报
J. Infrared Millim. Waves

Vol. 45, No. 1
February, 2026

文章编号：1001-9014(2026)01-0030-06

DOI:10.11972/j.issn.1001-9014.2026.01.004

High performance multifunction integrated optic circuits base on thin-film lithium niobate

QU Bai-Ang[1,2], GUO Hong-Jie[3,4], YANG Yong-Kang[1,2], CHEN Wen-Bin[1,2], ZHANG Xue-Chen[1,2], GUO Wen-Tao[2*], TAN Man-Qing[1,2*]

(1. School of Materials Science and Optoelectronic Technology, University of Chinese Academy of Sciences, Beijing 100049, China;
2. National Key Laboratory of Optoelectronic Materials and Devices, Institute of Semiconductors, Chinese Academy of Sciences, Beijing 100083, China;
3. Innovation Academy for Microsatellites, Chinese Academy of Sciences, Shanghai 201304, China;
4. Shanghai Engineering Center for Microsatellites, Shanghai 201210, China)

Abstract: This paper introduces an innovative Multifunction Integrated Optic Circuit (MIOC) design utilizing thin-film lithium niobate, surpassing traditional bulk waveguide-based MIOCs in terms of size, half-wave voltage requirements, and integration capabilities. By implementing a sub-wavelength grating structure, we achieve a Polarization Extinction Ratio (PER) exceeding 29 dB. Furthermore, our electrode design facilitates a voltage-length product ($V_\pi L$) below 2 V·cm, while a double-tapered coupling structure significantly reduces insertion loss. This advancement provides a pivotal direction for the miniaturization and integration of optical gyroscopes, marking a substantial contribution to the field.

Key words: MIOC, thin-film lithium niobate, sub-wavelength grating, polarization extinction ratio

基于薄膜铌酸锂的高性能多功能集成光路

屈柏昂[1,2]，郭宏杰[3,4]，杨永康[1,2]，陈文彬[1,2]，张学琛[1,2]，郭文涛[2*]，谭满清[1,2*]

(1. 中国科学院大学 材料科学与光电技术学院,北京100049;
2. 中国科学院半导体研究所 光电子材料与器件全国重点实验室,北京100083;
3. 中国科学院微小卫星创新研究院,上海201304;
4. 上海微小卫星工程中心,上海201210)

摘要:文章介绍了一种前沿性的多功能集成光路(Multifunction Integrated Optic Circuit ,MIOC)设计,该设计基于薄膜铌酸锂,在尺寸、半波电压要求和集成能力方面超越了传统的基于体波导的MIOC。通过实施亚波长光栅结构,我们实现了超过29 dB的偏振消光比(Polarization Extinction Ratio, PER)。此外,我们的电极设计使电压长度积($V_\pi L$)低于2 V·cm,而双锥形耦合结构则显著降低了插入损耗。这一进步为光学陀螺仪的小型化和集成化提供了关键方向,标志着对该领域的重大贡献。

关 键 词:MIOC;薄膜铌酸锂;亚波长光栅;偏振消光比

中图分类号:TN25　　**文献标识码**:A

Introduction

The fiber-optic gyroscope (FOG) is one of the most successful fiber optic angular velocity sensors and has been used across various platforms, such as aerospace, navigation, geological exploration, oil exploration, and earthquake monitoring[1]. The multifunction integrated optic circuit (MIOC) is a crucial optical component in the fiber optic gyroscope (FOG) as it is responsible for

Foundation items: Supported by Beijing Municipal Natural Science Foundation (424206); the Youth Innovation Promotion Association, CAS (2021108).
Biography: QU Bai-Ang(2000-), male, Shaanxi, Ph. D student. Research area involves Semiconductor optoelectronic devices and applications. E-mail: qubaiang@semi.ac.cn
* **Corresponding author**: E-mail: wtguo@semi.ac.cn; mqtan@semi.ac.cn

performing essential functions such as polarization filtering, light splitting, and phase modulation[2]. A highly efficient MIOC is paramount in achieving a FOG that is highly sensitive, compact, and easily integrated.

The MIOC is generally fabricated with the lithium niobate (LiNbO3) crystal because of advantages of large electro-optic coefficient, reliable physical and chemical characteristics[3]. Typically, the conventional MIOCs are obtained through the process of Annealing Proton Exchange (APE), which results in a naturally high extinction ratio[4]. However, its poor optical confinement ability leads to bulky modulators with low modulation efficiency ($V\pi L$ > 10 V·cm)[5]. In recent years, the thin film lithium niobate (TFLN) has emerged as a promising platform for excellent and compact electro-optic modulator due to its advantages of low optical loss, ultrafast modulation and high modulation efficiency ($V\pi L$ < 1.5 V·cm)[6-8].

However, the fabrication of TFLN-based optical waveguides technically have the challenge of high polarization extinction ratio[9]. Researchers have explored various solutions, such as sub-wavelength gratings[10-11], evanescent coupling[12-13], and multimode interference (MMI)[14-15], to address this issue. However, the results of these approaches have not met the requirements for applications such as fiber optic gyroscopes. Up to now, it is still a challenge to design MIOC with low optical loss, high modulation efficiency, and high extinction ratio in a small footprint, simultaneously.

Here, we introduce a novel design approach for Multifunction Integrated Optic Circuits (MIOC) utilizing thin-film lithium niobate, which, to our knowledge, is unprecedented. This design achieves a high polarization extinction ratio (PER) through the implementation of a sub-wavelength grating scheme, in conjunction with a carefully designed ridge waveguide that ensures single-mode operation. To minimize optical loss, a double-layer anti-taper coupling structure has been developed. The resulting MIOC demonstrates superior performance, including a high PER (exceeding 29 dB), a low half-wave voltage (V_π less than 2 V), and a compact form factor (less than 2 cm), distinguishing it from traditional MIOC designs. The insights gained from this work significantly advance to advancing the development of high-performance MIOC devices.

1 Design and simulation

The proposed MIOC is designed on a 400-nm X-cut LNOI platform, with light propagation primarily along the optical axis (Y-axis). A schematic diagram of the device is presented in Fig. 1. The structure integrates three double-layer anti-taper couplers, a subwavelength grating, and two phase modulators. The double-layer couplers are implemented to minimize optical loss, while the subwavelength grating is incorporated to enhance the polarization extinction ratio (PER). The two phase modulators are used to modulate the optical signals in the two branches, both of which share the same ground-signal-ground (GSG) electrodes. The operational principles and performance characteristics of the proposed device are analyzed and discussed in the subsequent sections.

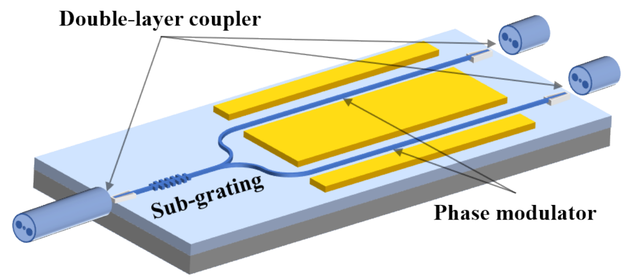

Fig. 1 MIOC structure diagram
图1 MIOC结构图

1.1 Single-mode

The modulation structure is formed by ridge waveguides and cladded by air (Fig. 2(a)). The sidewall angle is set to 65° according to our LNOI etching process. The main structural parameters are the rib width and the rib height, we evaluate the mode cut-off condition of the ridge waveguide using the Finite Difference Eigenmode (FDE) solver. Figure 2(b) presents a result heatmap illustrating the relationship between the allowable modes of the ridge waveguide and variations in rib width and rib height. The horizontal axis represents the rib width, while the vertical axis corresponds to the rib height. The color gradient depicts the mode cutoff characteristics, with distinct regions indicating the conditions under which specific modes are supported. The results reveal that as both rib width and rib height increase, the mode cutoff condition transitions from supporting only the TE mode (region I) to supporting both the TE and TM modes (region II). It is also apparent that the condition supporting only the TE mode is more easily achieved under shallow etching, albeit at the cost of higher propagation losses. Considering these factors, a rib width of 0.8 μm and a rib height of 0.2 μm were chosen. Under these parameters, the ridge waveguide supports only the TE mode (region I in Figure 2(b)), while the TM mode is effectively cut off and primarily radiated into the Si substrate.

1.2 Sub-grating

Subwavelength gratings (SWGs), comprising periodically arranged dielectric segments with a pitch significantly smaller than the wavelength of incident light, have been extensively studied as a means to develop high-performance integrated photonic devices characterized by compact size, low optical loss, and broad operational bandwidth.

Figure 3(a) illustrates the schematic diagram of the proposed SWG-based TE-mode-pass filter. Based on the preceding analysis, the thickness of the SWG structure is also set at 200 nm to ensure robust mode confinement within the lithium niobate slab. For this TE-mode-pass filter, the hybrid SWG waveguide operates in the Bragg regime for the TE mode and in the subwavelength regime for the TM mode. Consequently, the incoming TM mode

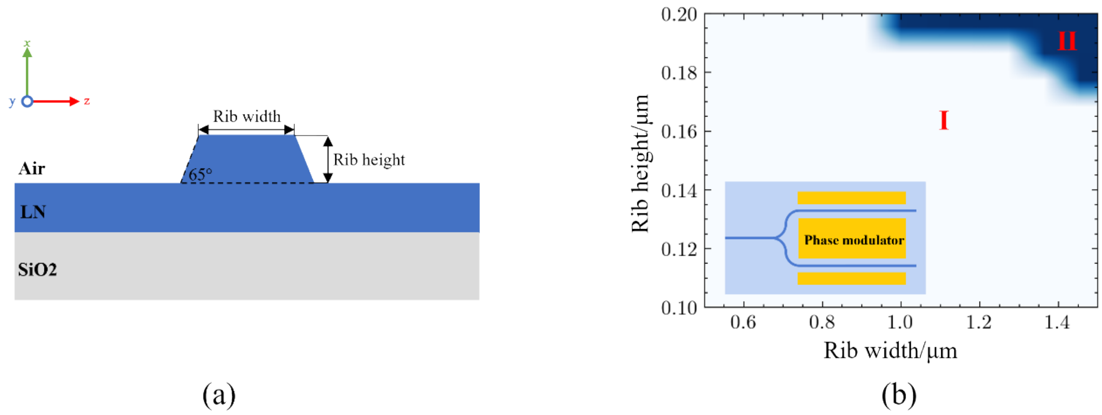

Fig. 2 (a) Lithium niobate thin film simulation model; (b) Single mode condition heat map
图2(a) 铌酸锂薄膜仿真模型;(b)单模条件热力图

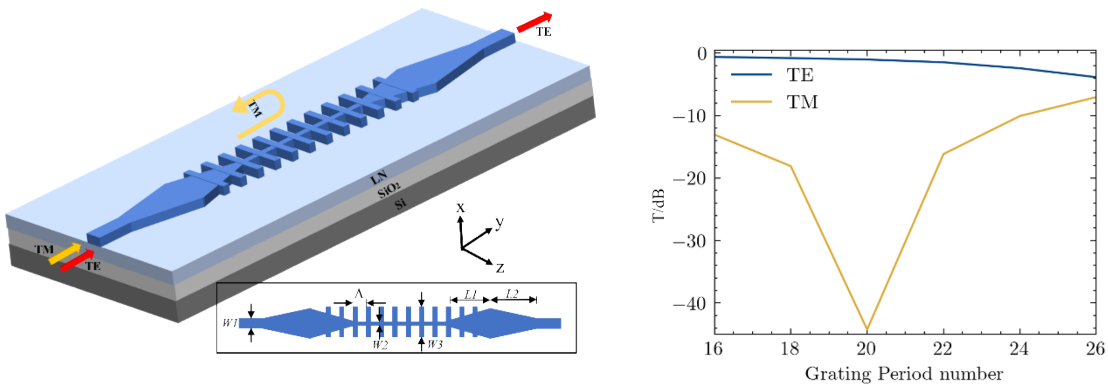

Fig. 3 (a) The schematic diagram of SWG; (b) SWG simulation extinction ratio results
图3 (a)SWG示意图;(b)SWG模拟消光比结果

is reflected, while the TE mode transitions into a localized Bloch mode and propagates with minimal loss [16].

$$\Lambda = \frac{\lambda}{2 \cdot n_{eff_{TM}}} > \frac{\lambda}{2 \cdot n_{eff_{TE}}} , \tag{1.1}$$

where Λ is the grating pitch, λ is the central wavelength of photonic stop band for TE mode, n_{TE} and n_{TM} are the effective indices of TE and TM modes in the SWG waveguide.

The SWG structure is optically equivalent to a homogeneous medium with a refractive index given by[17]:

$$n_{SWG}^2 = n_{LN}^2 \cdot f + n_{air}^2 \cdot (1 - f) , \tag{1.2}$$

where n_{LN} and n_{air} are the refractive indices of lithium niobate and air clad, respectively. The f is the filling factor of the SWG, which is expressed as $f = W/\Lambda$ where W_t is the width of the SWG segment. Here, the f is designed to be 0.8, for an easy-to-fabricate minimum feature size.

Then, the effective refractive indices of the Bloch modes in the SWG waveguide are calculated by using a Finite Difference Eigenmode solver. The parameters in the SWG structure are designed to be W_1=0.8 μm, W_2=0.3 μm, W_3=2 μm, L_1 = L_2 =5 μm, Λ=456 nm, W_t=364.8 nm . The transmission of TE and TM modes as a function of grating period number is simulated at a wavelength of 1 550 nm, by using the 3D finite-difference time-domain (3D-FDTD) method, as shown in Figure 3b. To achieve both low loss and high polarization extinction ratio (PER), the grating period number is chosen to be 20. The simulated insertion loss for TE mode is 0.8 dB and the PER is about 42 dB.

1.3 Double-coupler

The coupler is designed to couple with an PANDA polarization maintaining (PM) fiber with mode field diameter (MFD) of 6.5 μm. A cladding SiO_2 layer with 3 μm covers the whole taper area deposited by PECVD (Cladding SiO_2 is transparent in Fig. 4). The coupling loss includes the power coupling loss at region Ⅰ (in fig4. a) as well as the mode conversion loss from region Ⅰ to region Ⅳ (in fig. 4a). The cross-section view and corresponding mode field distribution of at different region of the coupler are shown in Fig. 4(b).

We use the Finite Difference Eigenmode (FDE) solver to simulate the coupling loss between the PM fiber and the coupler by optimizing the w_1 parameter. As shown in Figure 5a, the simulation result indicates that the coupling loss at region Ⅰ is about 0.4 dB. The, we use the Eigenmode Expansion (EME) solver to simulate the mode conversion loss between the region Ⅰ and region Ⅳ by optimizing the main parameter L_l as Fig5(b) shows. To minimize the coupling loss and the footprint of the coupler, we set the L_l to be 200 μm. Finally the coupling loss of 0.4 dB per facet is obtained for TE light in

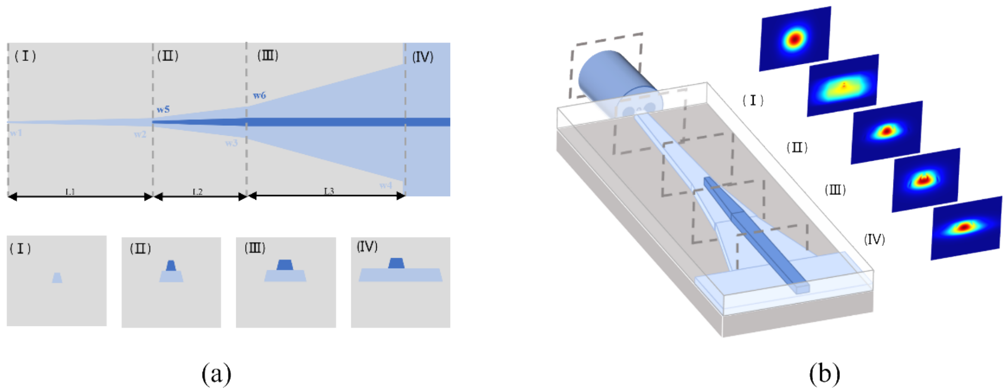

Fig. 4 (a) Top view of biconical coupling structure; (b) 3D diagram of bipyramidal coupling structure
图4 (a)双锥耦合结构顶视图;(b)双锥耦合结构三维图

simulations after optimization. The optimized values are listed in the Table 1.

2 Fabrication and measurement

For the fabrication of devices, we utilized 400 nm-thick lithium niobate thin films acquired from NANOLN, with a silica layer thickness of 4.7 μm. The fabrication process for the biconical coupling structures involved intricate steps, including two rounds of electron beam lithography (EBL) and two cycles of inductively coupled plasma reactive-ion etching (ICP-RIE). The ICP-RIE was conducted at powers of 600 W for the source and 100 W for the bias, using pure argon as the etching gas, and achieving a ridge angle of 65°. For the electrode structures, a magnetron sputtering technique was employed to deposit 50 nm of Ti and 300 nm of Au. The Ti layer served to mitigate absorption losses that could arise from direct contact between the Au metal and the waveguides. The desired metal patterns were then formed using ultraviolet lithography. Finally, the waveguides were cleansed with a solution of H_2O_2 to H_2SO_4 in a 3:1 ratio for 10 minutes to remove surface impurities. The device structure is illustrated in the figures provided. Figure (a) depicts the sub-wavelength grating test structure, where the deep green image represents the sub-wavelength grating structure as observed under an electron microscope. Figure (b) showcases a three-dimensional model of the biconical coupling structure, while figure (c) presents a top view of the biconical coupling structure.

Building on previous work[18], the measurements were conducted using a Santec TSL-570 tunable laser as the light source and a Santec PEM-340 polarization extinction ratio meter, operating in the 1 550 nm wavelength range. Under the TE single-mode condition, the waveguide achieved a polarization extinction ratio (PER)

Table 1 Double layer inverse cone coupler parameter list
表1 双锥耦合器参数表

Parameter	value	Parameter	value	Parameter	value
L_1	200 μm	L_2	50 μm	L_3	50 μm
w_1	0.19 μm	w_2	1.3 μm	w_3	1.5 μm
w_4	5 μm	w_5	0.15 μm	w_6	0.8 μm

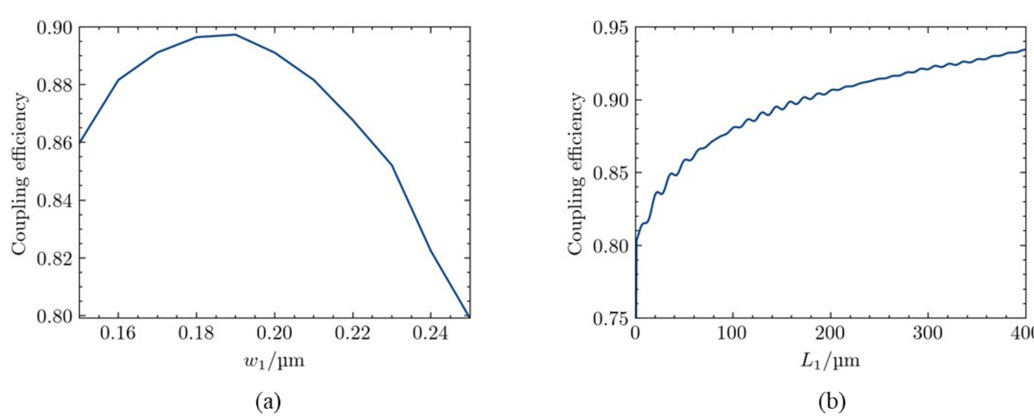

Fig. 5 (a) Relationship between w_1 and coupling efficiency; (b) Relationship between L_1 and coupling efficiency
图5 (a)w1与耦合效率关系;(b)L1与耦合效率关系

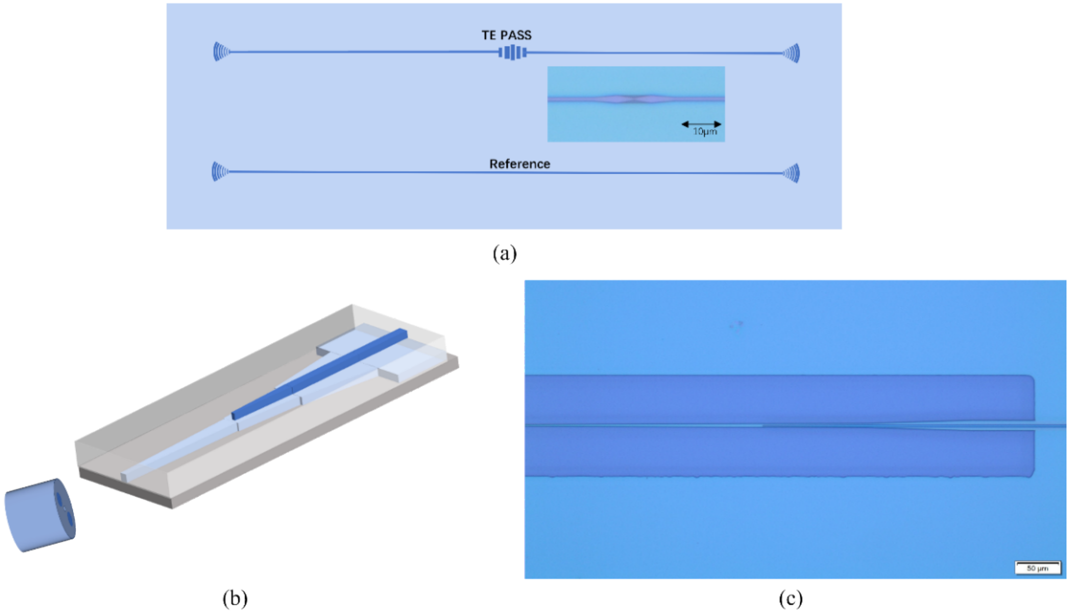

Fig. 6 (a) Test SWG Performance Structure; (b) Three-dimensional schematic diagram of coupling structure; (c) Coupled structure electron microscopy
图6 (a) SWG测试结构;(b)耦合结构三维示意图;(c)耦合结构电镜图

of 15 dB. By incorporating sub-wavelength grating structures, the PER was further improved. The experimental results, as shown in Fig8, reveal that the TE-pass sub-wavelength gratings achieved a PER exceeding 29 dB at 1 550 nm, outperforming polarization control methods previously reported for thin-film lithium niobate devices. Furthermore, at 1 530 nm, the PER reached nearly 40 dB, highlighting the superior polarization performance of sub-wavelength gratings and their wide spectral operating range. These results demonstrate the potential of sub-wavelength gratings to significantly enhance the functionality and application scope of thin-film lithium niobate Y-junction waveguide chips.

The half-wave voltage was tested as the system in Fig. 7(b), using a Santec TSL-570 tunable laser, voltmeter, MZI chip, and YOKOGAWA AQ6370D optical spectrum analyzer. The results indicate that with an electrode distance of 14 μm, the half-wave voltage is 6 V, and reducing the electrode gap to 7 μm lowers the half-wave voltage to 2 V. This phenomenon is consistent with theoretical expectations, where the electrode spacing plays a significant role in relation to the half-wave voltage. The facet structures introduce considerable coupling losses during testing, resulting in an overall device insertion loss greater than 10 dB. The high losses are attributed to two main factors: the complexity of the fabrication process, with a minimum etch linewidth of 190 nm, where the precision of the process significantly affects waveguide losses, and the use of large mode field diameter fibers (6 μm mode field diameter) for testing.

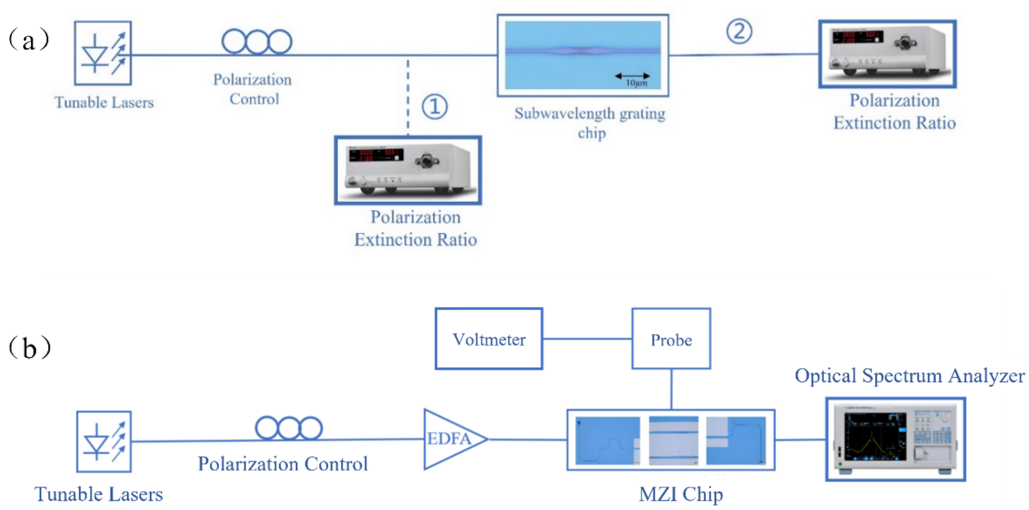

Figure 7 (a) Polarization extinction ratio test system[18]; (b) Half-wave voltage test system
图7 (a) 偏振消光比测试系统;(b) 半波电压测试系统

Previous reports of lower coupling losses were achieved by coupling thin-film lithium niobate to fibers with smaller mode fields (3 μm mode field diameter)[19]. Addressing the challenge of coupling to large mode fields remains a key issue in research. Future improvements may involve utilizing silicon nitride auxiliary schemes to enhance coupling efficiency.

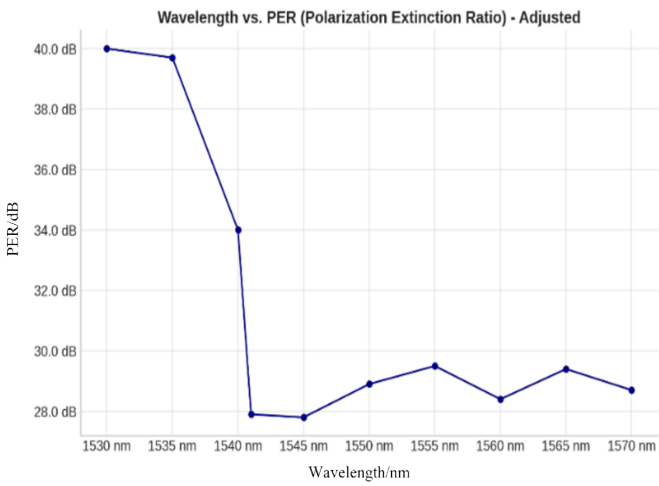

Fig. 8 Wavelength and extinction ratio test data
图8 波长及消光比测试数据

3 Conclusion

This paper introduces a novel design approach for Multifunction Integrated Optical Circuits (MIOC) based on thin-film lithium niobate, with a focus on key performance metrics including loss, half-wave voltage, and polarization extinction ratio (PER). Essential device designs were proposed and experimentally validated. To minimize losses, a dual-layer inverted taper structure was developed to reduce coupling losses. For controlling the half-wave voltage, adjustments to electrode spacing and structure achieved a half-wave voltage of less than 2 V, ensuring optical compatibility with CMOS processes—an important consideration for future photonic integration. Regarding PER control, an innovative approach using subwavelength gratings was introduced to enhance PER, achieving values greater than 29 dB at 1550 nm. This technique not only benefits MIOCs but also offers broader applicability for other systems requiring polarization management.

The proposed solutions represent a significant advancement in the application of thin-film lithium niobate to fiber optic gyroscopes, with both theoretical and experimental validation. This research opens valuable avenues for future work, particularly in optimizing the coupling compatibility between thin-film lithium niobate and large mode field fibers. The findings of this study are expected to significantly contribute to the development of compact, integrated optical gyroscopes.

References

[1] Passaro V M N, Cuccovillo A, Vaiani L, et al. Gyroscope Technology and Applications: A Review in the Industrial Perspective[J]. Sensors, 2017, 17(10): 2284.
[2] Lefevre H C, The fiber-optic gyroscope[M]. Artech house, 2022.
[3] Zhu D, Shao L, Yu M, et al. Integrated photonics on thin-film lithium niobate[J]. Advances in Optics and Photonics, 2021, 13(2): 242-352.
[4] Yu J, Zhang C, Li C, et al. Influence of polarization-dependent crosstalk on scale factor in the in-line Sagnac interferometer current sensor[J]. Optical Engineering, 2013, 52(11): 117101.
[5] Liu H F, Guo H J, Tan M Q, et al. Research progress of lith-ium niobate thin-film modulators[J]. Chinese Optics, 2022, 15(1): 1-13 (刘海锋,郭宏杰,谭满清,等. 铌酸锂薄膜调制器的研究进展[J]. 中国光学(中英文)),2022,15(1):1-13.
[6] Chen G, Li N, Ng J D, et al. Advances in lithium niobate photonics: development status and perspectives[J]. Advanced Photonics, 2022, 4(3): 034003.
[7] Luo Q, Bo F, Kong Y, et al. Advances in lithium niobate thin-film lasers and amplifiers: a review[J]. Advanced Photonics, 2023, 5(3): 034002.
[8] Guo H J, Liu H F. Design of a novel Y-junction electro-optic modulator based on thin film lithium niobite[J]. Journal of Infrared and Millimeter Waves, 2022, 41(3): 626-630.
[9] Liu J, Zhang C, Gao F, et al. Method for improving the polarization extinction ratio of multifunction integrated optic circuits[J]. Optics Express, 2021, 29(18): 28096-28103.
[10] Han X, Chen L, Jiang Y, et al. Integrated Subwavelength Gratings on a Lithium Niobate on Insulator Platform for Mode and Polarization Manipulation [J]. Laser & Photonics Reviews, 2022, 16 (7): 2200130.
[11] Han X, Jiang Y, Xiao H, et al. Subwavelength Grating-Assisted Contra-Directional Couplers in Lithium Niobate on Insulator[J]. Laser & Photonics Reviews, 2023, 17(10): 2300203.
[12] Chevriaux D, Khomeriki R, Leon J. Bistable transmitting nonlinear directional couplers[J]. Modern Physics Letters B, 2006, 20(10): 515-532.
[13] Dai D, Wang S. Asymmetric directional couplers based on silicon nanophotonic waveguides and applications[J]. Frontiers of Optoelectronics, 2016, 9(3): 450-465.
[14] Wang K, Dong X, Köhler M H, et al. Advances in Optical Fiber Sensors Based on Multimode Interference (MMI): A Review[J]. IEEE Sensors Journal, 2021, 21(1): 132-142.
[15] Pau A, Jeevaratnam K, Chen Y S, et al. The Multiple Mini-Interview (MMI) for student selection in health professions training - a systematic review[J]. Medical Teacher, 2013, 35(12): 1027-1041.
[16] Halir R, Bock P J, Cheben P, et al. Waveguide sub-wavelength structures: a review of principles and applications[J]. Laser & Photonics Reviews, 2015, 9(1): 25-49.
[17] Cheben P, Halir R, Schmid J H, et al. Subwavelength integrated photonics[J]. Nature, 2018, 560(7720): 565-572.
[18] Yang Y K, Guo H J, Chen W B. High polarization extinction ratio achieved base on thin-film lithium niobate[J]. Journal of Infrared and Millimeter Waves, 2024, 43(6): 827 - 831.
[19] Yu Z, Yin Y, Huang X, et al. Silicon nitride assisted tri-layer edge coupler on lithium niobate-on-insulator platform[J]. Optics Letters, 2023, 48(13): 3367-3370.